JOURNAL OF THE AMERICAN WATER RESOURCES ASSOCIATION
DECEMBER AMERICAN WATER RESOURCES ASSOCIATION 2003

USE OF HEMISPHERIC IMAGERY FOR ESTIMATING STREAM SOLAR EXPOSURE[1]

Paul L. Ringold, John Van Sickle, Kristie Rasar, and Jason Schacher[2]

ABSTRACT: Solar exposure profoundly affects stream processes and species composition. Despite this, prominent stream monitoring protocols focus on canopy closure (obstruction of the sky as a whole) rather than on measures of solar exposure or shading. We identify a candidate set of solar exposure metrics that can be derived from hemispheric images. These metrics enable a more mechanistic evaluation of solar exposure than can be achieved with canopy closure metrics. Data collected from 31 stream reaches in eastern Oregon enable us to quantify and compare metrics of solar exposure from hemispheric images and a metric of canopy closure with a concave densiometer. Repeatability of hemispheric metrics is generally as good as or better than the densiometer closure metric, and variation in the analysis of hemispheric images attributable to differences between analysts is negligibly small. Metrics from the hemispheric images and the densiometer are typically strongly correlated, at the scale of an individual observation and for 150 m stream reaches, but not always in a linear fashion. We quantify the character of the uncertainty in the relationship between the densiometer and the hemispheric metrics. Hemispheric imagery produces repeatable metrics representing an important ecological attribute; thus those researching the effects of solar exposure on stream ecosystems should consider the use of hemispheric imagery. (KEY TERMS: solar exposure; instrumentation; meteorology/climatology; densiometer; hemispheric imagery; stream assessment.)

Ringold, Paul L., John Van Sickle, Kristie Rasar, and Jason Schacher, 2003. Use of Hemispheric Imagery for Estimating Stream Solar Exposure. Journal of the American Water Resources Association (JAWRA) 39(6):1373-1384.

INTRODUCTION

Solar input drives stream heating, primary production, periphyton species composition, fish life history strategies, and numerous other stream parameters (Gregory, 1980; Cummins *et al.,* 1984; Beschta *et al.,* 1987; Feminella *et al.,* 1989; Tait *et al.,* 1994; Shaw and Bible, 1996; Rutherford *et al.,* 1999; Grether *et al.,* 2001). Despite its significance, prominent stream monitoring protocols (e.g., Fitzpatrick *et al.,* 1998; Peck *et al.,* 2000) focus on canopy closure (the proportion of the sky which is obscured when viewed from a point) (see Jennings *et al.,* 1999) rather than on more direct measures of solar exposure (the amount of solar energy received per unit area per unit time) or shading (the proportion of solar energy that is blocked by vegetation and topography). One study (Platts and Nelson, 1989) illustrated the distinction in showing that measures of shade were better predictors of salmonid biomass than measures of canopy closure in streams in the intermountain West. This result suggests that the widespread focus on canopy closure may err in quantifying solar exposure and its effect on stream characteristics. Thus, methods to quantify solar exposure should be defined and evaluated for use in stream monitoring and assessment programs.

Davies-Colley and Payne (1998) compared nine tools for measuring stream shade. They concluded that "using fisheye photography potentially yields maximum information, but requires much offsite image processing. This method may become more popular when digital cameras are fitted with fisheye optics" (Davies-Colley and Payne, 1998:258). Since their article was prepared, not only have digital cameras become fitted with fisheye optics, but a new generation of software has become available that greatly simplifies the analysis of hemispheric images.

Good reviews of the use of hemispheric imagery for plant and forest ecology are available (Chazdon and Field, 1987; Rich, 1990; Roxburgh and Kelly, 1995). Several authors discuss the merits of direct

[1]Paper No. 02088 of the *Journal of the American Water Resources Association.* **Discussions are open until June 1, 2004.**

[2]Respectively, Ecologist and Environmental Statistician, Western Ecology Division, National Health and Environmental Effects Research Laboratory, Office of Research and Development, U.S. EPA, 200 S.W. 35th Street, Corvallis, Oregon 97330; 3235 N.W. Orchard, Corvallis, Oregon 97330; and Dynamac Corporation, 200 S.W. 35th St., Corvallis, Oregon 97330 (E-Mail/Ringold: ringold.paul@epa.gov).

and indirect measurement methods for measuring solar exposure (e.g., Rich, 1990; Davies-Colley and Payne, 1998; Jennings *et al.,* 1999). Direct measures of solar radiation are valuable, but they represent only the period of time when the measurements are taken; for stream assessments they would need to be compared against comparable and simultaneous measures at a nearby unobstructed location. In contrast, indirect estimates developed from single hemispheric images are valid for as long a period as the image is a valid representation of the quantity and location of features that obscure the sun. In general, the correlation between hemispheric metrics (an indirect method) and direct measures of light is good, particularly under more open canopies and when atmospheric conditions are properly evaluated (Whitmore *et al.,* 1993; Easter and Spies, 1994; Roxburgh and Kelly, 1995; Comeau *et al.,* 1998; Jennings *et al.,* 1999; Machado and Reich, 1999; Ferment *et al.,* 2001).

Given hemispheric imagery's proven track record and its potential to provide information on stream solar exposure, our goal is to evaluate its feasibility and characteristics as a tool for stream monitoring and assessment. These steps are key elements to the second and third of four steps suggested for ecological indicator evaluation (Jackson *et al.,* 2000; Fisher *et al.,* 2001).

We examine four issues in our analyses. First, we identify a set of candidate indicators of solar radiation that may be valuable for stream assessments. Second, we compare canopy closure estimates using a densiometer (an inexpensive and widely used device) (Fitzpatrick *et al.,* 1998; Peck *et al.,* 2000), which has been useful in explaining the status of instream resources (e.g., Herlihy *et al.,* 1998; Hill *et al.,* 1998; Bryce *et al.,* 1999; Pan *et al.,* 1999) and measures of candidate indicators derived from hemispheric images. Third, we characterize sources of error in the analysis of hemispheric imagery. We examine analyst error because numerous previous researchers (Rich, 1990; Whitmore *et al.,* 1993; Jennings *et al.,* 1999; Robison and McCarthy, 1999; Englund *et al.,* 2000; Engelbrecht and Herz, 2001; Hale and Edwards, 2002) note this potential source of error. We also examine sampling error, because its magnitude is the key to making quantitative design decisions about the use of any monitoring tool. Fourth, we examine the relationship between both analyst and sampling error on the one hand and canopy closure on the other hand.

The key remaining step for indicator evaluation is to determine if the candidate indicator adds value in terms of our understanding, assessments, or management actions.

STUDY AREA AND METHODS

Study Area and Sample Reaches

Data were collected from 31 wadeable stream reaches within the John Day and Lower Deschutes Basins in central and eastern Oregon, USA (approximately 44.6°N and 119°W). The stream reaches sampled were selected on a probability basis from the perennial stream network of the region using well-documented methods (Stevens, 1997; Stevens and Olsen, 1999). We sampled stream reaches during the summers of 2000 and 2001, 11 the first year and the remainder the second year. Most of the streams sampled (26 of the 31) were on public land. Streams ranged in Strahler order from 1 to 4, with a median of 2. The mean bankfull width of these streams was 4.8 m and ranged from 1.1 to 11.1 m. Stream elevation ranged from 700 to 1,700 m, with a median elevation of 1,300 m. Vegetation along these streams ranged from dense conifer forests with canopies completely closed over the stream to sparse grasses and shrubs with virtually no vegetative closure over the stream.

Field Methods

At each stream reach we collected paired hemispheric images and densiometer readings. These data were collected at the "exact" coordinates of the stream sample point specified in the random sample of the stream network. We also collected samples at 30 m increments (as measured through the stream thalweg) upstream for approximately 300 m. Each image collection represents a sample point; the collection of images at a location represents a stream reach. The data were collected at a height of about 1 meter over the surface of the water in the center of the stream thalweg. In addition, observations were collected at temperature loggers at the upper and lower ends of the study reaches. Densiometer readings and hemispheric images were collected on the same day. All reaches were sampled during full leaf out, and some reaches were also sampled before full leaf out. Quantification of canopy closure and shading is attributable to multiple layers of vegetation as well as topography and some elements of the stream bank.

Densiometer Readings. Densiometer readings were collected according to the stream center protocol in the EMAP field manual (Peck *et al.,* 2000), although our densiometer readings were taken at 1 m, the same height at which we collected hemispheric images. This method is similar to that used in

other field protocols (Platts *et al.,* 1983, 1987; Fitzpatrick *et al.,* 1998). A densiometer is a convex gridded mirror in which the canopy and sky are visible. Each reading is a count of the number of 17 grid points that are not open to the sky. Densiometer readings are taken in four directions relative to the flow of the stream – upstream, downstream, left, and right. The four readings are combined into a total densiometer reading for the sample point. The maximum possible total is 68.

Hemispheric Images. Hemispheric images were collected with a Nikon Coolpix 950 (firmware version 1.3) with an FC-E8 fish eye lens. The camera was leveled and oriented on a tripod to magnetic north, which was marked on the images with a fiber optic tube. Color images were collected with automatic exposure, high contrast, in manual mode, with normal lens setting, and normal resolution resulting in an image size of approximately 300 kB in a JPG file with 1:4 compression and 1,600 by 1,200 pixels. The field of view was manually maximized before each image was collected so that the entire hemispheric view was captured as shown in Figure 1. As in other studies, hemispheric images were taken without the sun directly in the image to ensure that images could be collected with the contrast and lighting required for image classification. Therefore, photos were usually taken at dusk, with some taken at dawn or on overcast days.

Hemispheric Image Analysis

All of the images were analyzed in Hemiview version 2.1 software (Delta-T Devices, 1998). Analysis in Hemiview or similar programs requires the following steps.

1. Specify the image orientation (true N), the portion to be analyzed, and the location of the reach (latitude, longitude, and elevation).

2. Specify assumptions about the analytical approach. We used the lens calibration provided by the vendor, a uniform overcast sky model (assuming that diffuse radiation comes equally from all directions), and divided the image into eight azimuth and 18 zenith zones. We assumed a solar constant of 1,370 Wm^{-2}, a transmission coefficient (the percentage of solar radiation transmitted through a unit atmosphere depth) of 0.8, and a diffuse proportion of 0.1.

3. Specify the nature and form of the desired output.

4. Classify the image (i.e., use a classification algorithm in the software to partition the image into pixels that block the sun and pixels that do not block the sun).

5. Calculate the metrics.

Image classification requires the analyst to partition the image into pixels that block the sun and pixels that do not. This is an iterative and subjective process in which the analyst makes a judgment about the classification as a whole. In about 4 percent of the cases we edited the images with either Adobe® Photoshop® (version 5.5) or Microsoft Photoeditor (version 3.01) before processing in Hemiview to obtain an acceptable classification. The edits were typically made to alter portions of the image that should have been classified as obscured but that were classified as visible. Although the sun was not in these images, portions of the image were classified as visible because the edited surface was still bathed in direct sunlight and was therefore too light to be classified properly.

Metrics Derived from Hemispheric Imagery. Hemispheric image analysis allows us to define a broad range of metrics. This includes the capacity to estimate potential solar exposure during any specified period of time for which the classified image is applicable. Our purpose is to examine the characteristics of a reasonable subset of this broad range of candidate metrics. These characteristics should be representative of the characteristics of other metrics that users may extract to reflect the facets of solar exposure appropriate for their work. We do not know which measures will be prove to be most closely linked with stream condition; thus ours is an initial list of candidates that we will modify by identifying which of these candidate metrics are most closely associated with stream condition (temperature patterns and metrics of periphyton, macroinvertebrate, and fish status).

Previous workers (e.g., Platts and Nelson, 1989) have examined and found value in using metrics of solar exposure for the entire year. However, in the temperate zone potential solar exposure varies by a factor of 5 or more from the winter months to the summer months. Therefore, it is appropriate to examine solar exposure for months that are plausibly linked to the ecological responses of interest. Beschta *et al.* (1987) note that for summertime stream temperature, the characteristic of sunlight that we wish to know is direct solar radiation during the middle four hours of the day. However, examination of temperature records of streams shows that maximum temperatures may be sustained for very short periods of

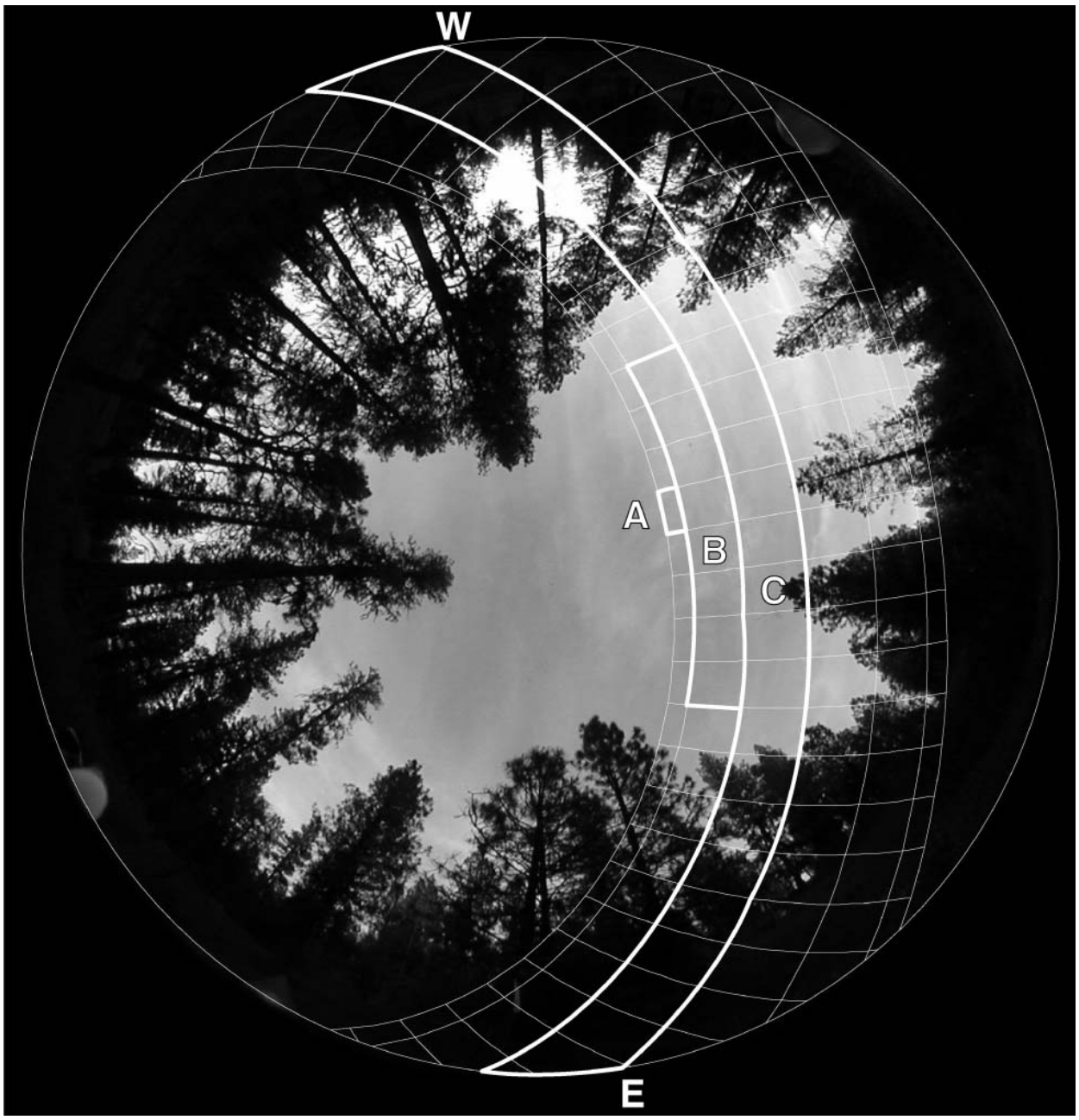

Figure 1. An Example of a Hemispheric Image. The area analyzed is within the circle. The semicircle on the lower left margin of the image is the fiber optic marker that denotes magnetic north. The grid is added by the software, Hemiview. The inner arc of the grid is the path of the sun on the day when it reaches the highest elevation during the course of the year (approximately June 21). The outer arc of the grid is the path of the sun on the day when it reaches its lowest elevation during the course of the year (approximately December 21). The area between the arcs describes the path of the sun during two months: the inner area is for June and July; the outer area is for December and January. The lines perpendicular to the arcs describe half-hour increments in the movement of the sun. The block labeled A is the portion of the sky that determines the metric MAXJune (see Table 1). The block labeled B is the portion of the sky that determines the metric MID4August. The block labeled C is the portion of the sky that determines the metric DAYSeptember. The full grid is the portion of the sky that determines DSF.

time, suggesting that we may wish to examine solar exposure for a correspondingly short period. In response to these considerations, we focus our analysis on nine metrics. These are a hemispheric measure of canopy closure (Vissky) and solar exposure for the year (DSF, ISF, and GSF). We select July as a month to focus on as a typical summer month. For July we evaluate measures of solar exposure for the entire day (DAYJuly), for the middle four hours of the day (MID4July), and for the maximum half-hour of the

day (MAXJuly). As a heuristic companion to these analyses we examine a measure of solar exposure for the entire day for the month of January (DAYJanuary), when the solar position is very different than in July, as shown in Figure 1. Finally, we examine LAI because other users may find this analysis of value.

Table 1 provides more detailed definitions of the metrics that we have chosen to examine. It also illustrates that the set we examine are a subset of a larger number of metrics that could be used in assessing stream habitat. The portions of the sky whose cover determines direct solar exposure for various time periods are identified in Figure 1.

Estimates of the amount of direct radiation are listed as potential estimates because we specify fixed assumptions about atmospheric conditions and canopy closure. This is the same approach that has been taken in other analyses (e.g., Platts *et al.,* 1987; Platts and Nelson, 1989; Maloney *et al.,* 1999). Providing estimates of the actual amount of radiation received would require modification of potential values by atmospheric data such as those in the Agrimet network (U.S. Bureau of Reclamation, 2001). This regional adjustment, however, would not adjust the potential estimates to reflect differences in light quality, i.e., shifts in wavelength that result from canopy structure and composition, and cloud cover (e.g., Lieffers *et al.,* 1999; Rutherford *et al.,* 1999).

Data Analysis

We use different subsets of our data for different purposes. A summary and characterization of the points where these sets of images were collected is provided in Table 2.

Relationship Between Closure and Shade. We evaluate the relationship between metrics derived from densiometer readings and those from hemispheric imagery at both point and reach scales using datasets D and E (Table 2). At the reach scale, metrics are the average of measurements over the first 150 m of the stream reach. We selected 150 m because this enables us to conduct our analysis with a single standard length, which is the length of an EMAP sample reach for streams up to 3.75 m in bankfull width (Peck *et al.,* 2000). At the reach scale, we used only samples taken during full leaf out. We weighted multiple observations taken from the same point as if we had collected only one measure at that point.

Scatter plots of the relationship between hemispheric metrics and densiometer total were examined. When the best fit did not appear to be linear, examination of the scatter plot suggested alternative transformations (e.g., a cubic fit as shown in Figure 2b). We quantify the uncertainty in the relationship by reporting the R^2 values and by reporting the standard error of the regression prediction as a percentage of the regression prediction. This percentage varies over the range of canopy closure, so we report the value for more open canopies, average canopies, and more closed canopies. We also illustrate the magnitude of the uncertainty by providing scatterplots that include regression lines and 95 percent confidence intervals for individual predictions.

Analyst Error and Software Differences. We selected 31 images to evaluate the sensitivity of the

Table 1. List of metrics derived from hemispheric images. We examined a subset of these metrics in this paper. Each metric can be expressed either at either the point or the reach scale. Definitions are from or are adapted from (Delta-T Devices 1998). Radiation estimates are for a horizontal intercepting surface. See Figure 1 for an illustration of which portions of the sky are associated with each of the direct radiation metrics. Months are generally defined as the period from the 22 of the previous month through the 21 of the current month. Units of radiation are in Mega joules per meter square per unit time.

Metric Category	Abbreviation	Description
Visible Sky	Vissky	The proportion of pixels which are classified as visible sky.
Site Factors	DSF, ISF, GSF	The proportion of direct, indirect, or total solar radiation reaching a point relative to that in a location with no sky obstructions.
Monthly Direct Solar Radiation	DAYmonth	The potential direct radiation received below the canopy for each month.
Maximum Direct Solar Radiation	MAXmonth	The potential maximum amount of direct radiation received below the canopy during any half hour period during each month.
Mid Day Direct Solar Radiation	MID4month	The potential amount of direct radiation received below the canopy between 10 a.m. and 2 p.m. during each month.
Effective Leaf Area Index	LAI	Half of the total leaf area per unit ground area. Assumes a random distribution of canopy elements; an assumption whose validity varies by stand types (Chen *et al.,* 1997).

Table 2. Characteristics of the different sets of point scale observations used in this analysis. Five images in dataset A are included in dataset B; all of dataset B images are included in dataset C; half of dataset B is included in datasets E, and 24 of dataset A images are included in dataset E. Dataset E is aggregated to the reach scale. The pairs of samples included in B and C were all taken during the period of full leaf out. The average time between the repeat measurements was 67 days ranging from 47 to 90 days.

	Data Set				
	A	**B**	**C**	**D**	**E**
Purpose	Image Classification Error	Sampling Error Point Scale	Sampling Error Reach Scale	Relationship to Densiometer Readings	150 m Reach Characterization
Number of Observations	31 Sample Points	33 Pairs of Sample Points	9 Sample Reaches	557 Sample Points	218 Sample Points
Selection and Use	Stratified Probability Selection From First 143 Images From 10 Reaches	Repeat Observations at 33 Points on 9 Reaches	Repeat Reach Scale Observations at 256 Points From 9 Reaches	All Observations From 31 Reaches	Observations From a Single Visit for the First 150 m of 31 Reaches
			Densiometer Total		
Minimum	1	12	2	0	0
Mean/SD	33/18	42/15	38/15	36/19	34/21
Maximum	59	68	68	68	68

results of image classification to the varying judgment of multiple analysts. To ensure that these images covered a broad range of canopy conditions, we selected the images at random from nine strata defined by three levels of densiometer total (0 to 25, 26 to 43, and 44 to 68) and by three levels in the range of the four densiometer readings that comprise the total densiometer reading (0 to 4, 5 to 10, and 11 to 17). The sample was drawn from the set of 143 images collected early in the first year of study.

Seven analysts – four experienced and three inexperienced – classified each of the 31 images (see Dataset A in Table 2). For each image and analyst we calculated the candidate indicators listed in Table 1.

We compared the variability in metrics attributable to analysts (VA) to the variability across the images (VI). We assumed a random effects model for both the effect of the analyst and the effect of the image on the metric value. Components of variance were then estimated for each of the two effects using standard methods (Miller, 1986). We also examine the ratio VA/VI not only for the full dataset, but also within eight subsets of the data: experience level of the analyst (experienced and inexperienced), densiometer total (three subsets), and densiometer range (three subsets). Finally, we examine the correlations and regressions for five metrics (Visible Sky; Direct, Indirect, and Global Site Factor; and LAI) derived from these 31 images in two additional software packages – Winscanopy® (Regent Instruments, 1999) and GLA (Frazer *et al.,* 1997).

Sampling Error. We characterize sampling error during the full leaf out period. We characterize sampling error at the point scale by evaluating pairs of repeat measurements at 33 individual well located points from nine stream reaches (Dataset B in Table 2). We characterize sampling error at the reach scale by evaluating pairs of repeat measurements at the same nine stream reaches (Dataset C in Table 2). Sampling error is quantified in the form of the standard deviation, s, and as CV*, the coefficient of variation with a correction for bias (Sokal and Rohlf, 1981). To evaluate the possibility that either analyst or sampling error is a function of canopy opening we compare s for each type of error as a function of canopy closure as measured with a densiometer. Our evaluation of the correlations includes a Bonferroni correction for comparisons across the nine metrics that we evaluate.

Statistical analyses were conducted with SPSS® version 10 and higher, SAS® 8.2, and Microsoft® Excel 2000. The calculation of CV* was the only statistical calculation done in Excel. These calculations were verified for accuracy, in a few cases, using SPSS.

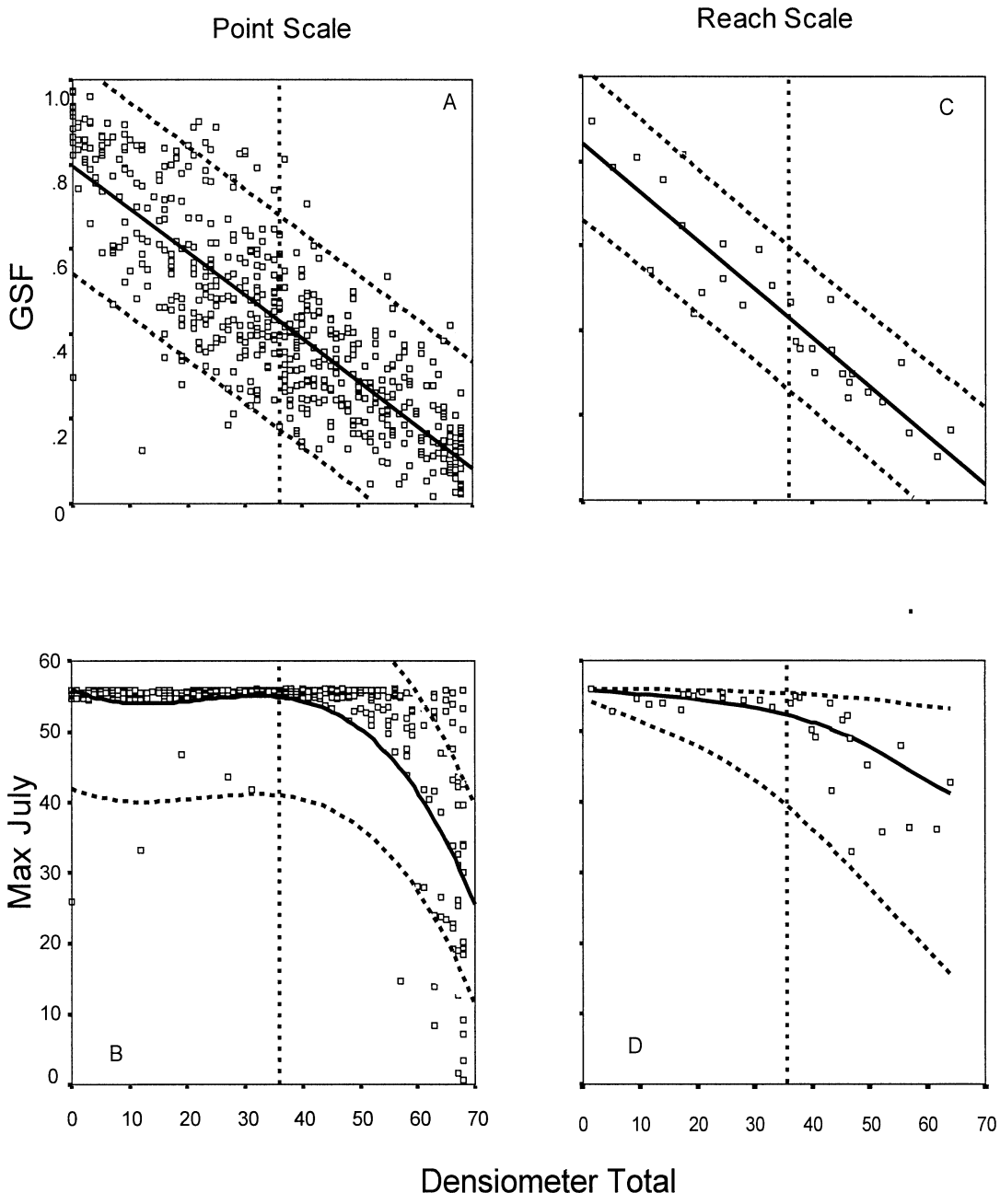

Figure 2. Examples of the Associations between Densiometer Readings (the x-axis) and Two Metrics from Hemispheric Images. Figures 2A and 2B are for the point scale; 2C and 2D are the same metrics on the same axes for the reach scale. The heavy black lines represent the least squares regression lines. The form of the fit is provided in Table 3. The pair of dashed lines that roughly parallel the regression lines represent the 95 percent confidence intervals for individual predictions. The vertical dashed lines show the average densiometer reading. Definitions of the metrics are provided in table titles in Table 1.

RESULTS

Relationship Between Hemispheric Metrics and Densiometer Readings

There is a strong correlation between densiometer readings and hemispheric metrics at the point and reach scales (Figure 2 and Table 3). The R^2 for the reach scale regressions are about one-third larger than the corresponding R^2 at the point scale. The correlation is stronger for metrics that have a smaller directional component and weaker for metrics that have a directional component, especially when that directional component is at a low zenith angle. For

Table 3. The Relationship Between Densiometer Total (X) and Metrics From Hemispheric Imagery (Y). Descriptions for hemispheric metrics are as provided in Table 1. For the linear form $Y = b_0 + b_1*(X)$; for the log form $Y = b_0 + (b_1*\ln(x))$ for the logistic form $Y = u/(1 + b_0 + b_1^x)$; b_0, b_1 and u are fit in the regression model. In all cases $p < 0.01$ with a Bonferroni adjustment fir the significance of the correlation coefficient. There are 558 pairs of observations for all point scale analyses except for Leaf Area Index where it is 158; there are 31 pairs of observations at the reach scale. The uncertainty of the regression prediction (the standard error of the regression prediction/regression prediction) is provided for three levels of densiometer reading. These are the 10th percentile, the mean, and the 90th percentile of Dentotal for each dataset.

	Point Scale					Reach Scale				
			Standard Error of Regression Prediction/Regression Prediction at Dentotal =					Standard Error of Regression Prediction/Regression Prediction at Dentotal =		
Hemispheric Metric (Y)	Form	R^2	9	36	63	Form	R^2	10	34	57
Vissky	Linear	0.78	15%	25%	76%	Linear	0.89	10%	16%	40%
DSF	Linear	0.66	20%	32%	93%	Linear	0.84	12%	20%	48%
GSF	Linear	0.69	18%	30%	84%	Linear	0.86	11%	18%	43%
ISF	Linear	0.82	12%	19%	50%	Linear	0.94	7%	10%	21%
DAYJan	Log(X)	0.30	59%	140%	329%	Log(X)	0.53	39%	92%	353%
DAYJuly	Linear	0.68	18%	28%	69%	Linear	0.89	9%	14%	29%
MAXJuly	Cubic	0.52	13%	12%	19%	Logistic	0.60	9%	9%	12%
MID4July	Linear	0.55	21%	31%	63%	Linear	0.81	11%	16%	28%
Ln(LAI)	Linear	0.65	63%	179%	37%	–	–	–	–	–

example, at the point scale, the R^2 for DSF is lower (at 0.66) than the R^2 for ISF (at 0.82), and the R^2 for DAY is lower during January (0.30) than during July (0.68). The correlation is also larger when a longer period of the day is examined. For example, correlations are greatest for the full day in July, smaller for the middle four hours, and smallest for the maximum half-hour.

The magnitude of the prediction standard error in relation to the regression prediction varies with the canopy closure. Except for LAI, the relative magnitude of the prediction uncertainty usually increases by a factor of two to four or more as canopies become more closed (Table 3).

Variability in Image Classification

Image classifications by different people lead to different estimates of each metric (Figure 3). If the variability in a metric attributable to classifications produced by different analysts (VA) is small relative to the variability in a metric attributable to different locations (VI), then analyst differences can be ignored. The average value of VA/VI for all nine metrics, 0.08 percent, is very small. Even the maximum value of this ratio, 0.22 percent for LAI, is very small. We also

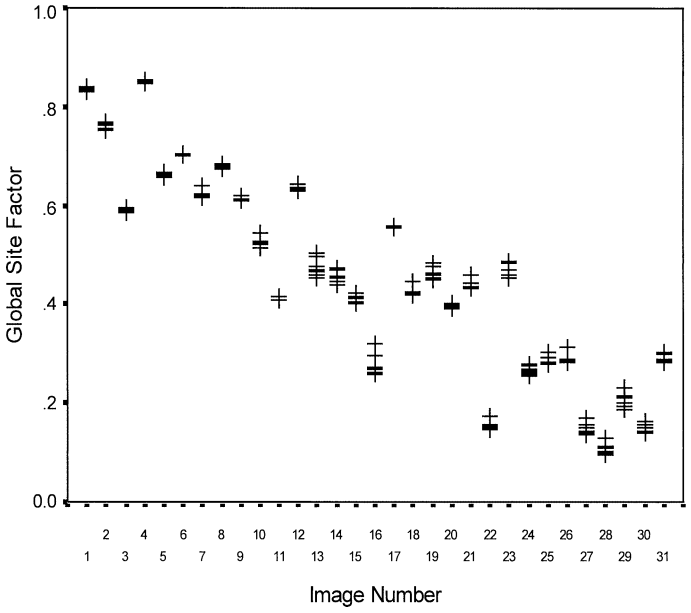

Figure 3. Estimates of Global Site Factor by Each of Seven Analysts for Each of 31 Images. The images are ordered by densiometer total, which ranges from one for Image 1 through 59 for Image 31. Compare the spread of estimates for each image to the width of the confidence interval shown in Figure 2A.

examine this ratio within subsets of the data: experience level of the analyst, densiometer total, and densiometer range. The average ratio in the subsets is always less than 1 percent except for four metrics in one subset of the data – Vissky (2.1 percent), ISF and Difbe (both 3.1 percent), and LAI (1.8 percent) in the high densiometer total subset. Thus, we conclude that analyst error is negligible.

Software Similarities. For Visible Sky, Direct, Indirect, and Global Site Factor, the predictions of all three software packages were very similar, with Rs values greater than 0.990, regressions slopes very close to 1, and intercepts very close to 0. For LAI, while the correlations were still quite high, there were substantial differences from a slope of 1 and an intercept of 0 in the regressions. These differences are attributable to clearly stated differences in the definition of LAI across the three programs.

Sampling Error

Metrics derived from hemispheric imagery have sampling error comparable to those for densiometer total, the metric derived from a densiometer, except for DAYJanuary (Figure 4). Errors for metrics that reflect annual exposures (GSF, ISF, and DSF) are lower than errors for metrics of direct monthly exposures (DayJan and DayJuly). For July, errors are smallest for the maximum half-hour (MAXJuly metric); the sampling errors for the whole day or for the middle four hours are equivalent. The largest sampling error is for DAYJanuary. Sampling error is an order of magnitude larger than analyst error, because analyst error is a subcomponent of sampling error. There is a small number of outliers and extreme values (Figure 4) that in some instances arise from very small differences in sampling locations. Sampling errors are generally not correlated with Vissky at either the point or the reach scale.

DISCUSSION

The results presented here allow us to evaluate the feasibility and response variability guidelines for indicator evaluation (Cairns *et al.,* 1993; Jackson *et al.,* 2000; Fisher *et al.,* 2001).

Our image collection is evidence of the feasibility of collecting hemispheric images on wadeable streams. The time required to collect the images and the training requirements for field crews to secure usable images are minimal. The average time between images collected on a reach was 4.4 minutes, ranging from 1.5 to 9.8 minutes. The significant constraint on image collection is the requirement that the sun cannot be directly visible in the images. Thus a field crew can only plan to collect images over a short time per day. Hemispheric images require effort in the office to translate the images into metrics. We found that an experienced analyst can use the software to make this translation in less than three minutes per image, particularly when the images are from the same location. Our image processing rate is about the same as with earlier software (Rich, 1990; Whitmore *et al.,* 1993).

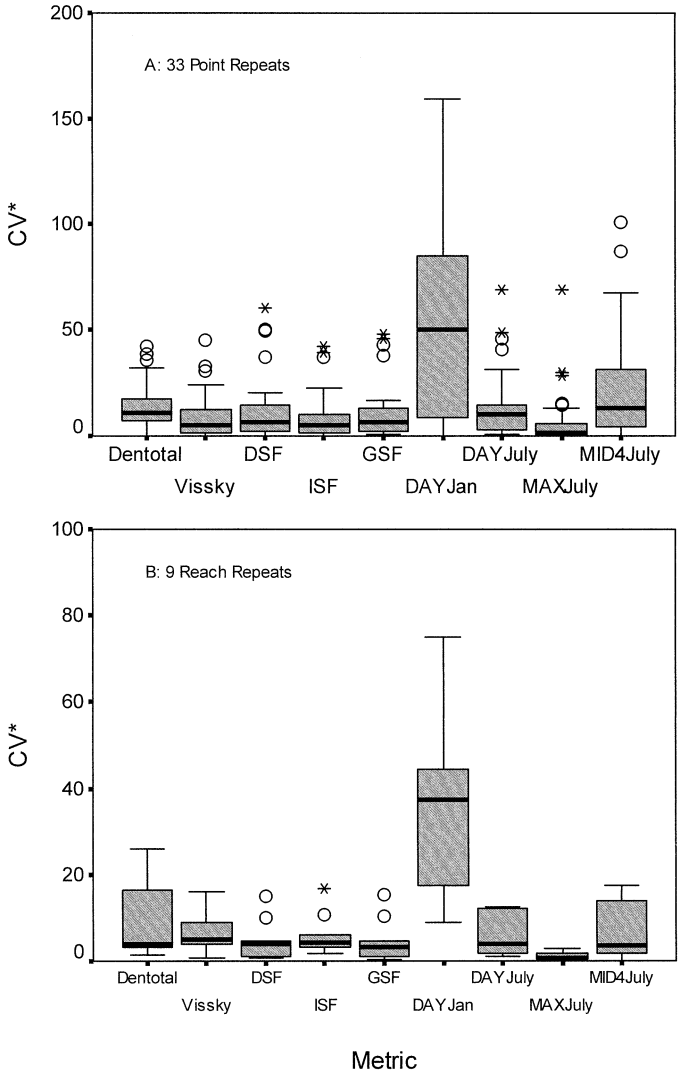

Figure 4. Sampling Error Associated with Different Measurement Technologies and Metrics at (A) the Point Scale and (B) the Reach Scale. The solid bar through each box is the median; the box depicts the interquartile range; ❍ is an outlier; and ∗ is an extreme value.

Error must be well characterized for an indicator to be useful. We examined two types of error. We conclude that analyst error is negligible, as did Robison and McCarthy (1999). Our result differs in that we used a digital rather than a film camera, examined a broader set of metrics, and based our conclusions on the relative magnitude of the analyst error (VA) as compared to the variability across the images (VI). We also found that experienced and inexperienced analysts gave similar results. Despite the negligibility of analyst error, a program that uses hemispheric imagery should include training and quality assurance with a fixed set of representative images to ensure and to document analyst consistency.

Sampling error for the ecologically relevant metrics derived from hemispheric images – those for the full year or for the summer months – is comparable to the sampling error of the densiometer metric. While some note that the "densiometer does not give a highly accurate measure of canopy closure" (Jennings *et al.,* 1999:67), others (e.g., Kaufmann *et al.,* 1999) compare the sampling error of densiometer measures to other measures used in characterizing stream habitat and conclude that densiometer sampling error is quite good relative to the sampling error of other indicators. Thus, the potential to provide information on an important stream process with relatively good sampling error makes hemispheric imagery a good candidate for further evaluation.

Hemispheric images can be collected with either film or digital technology. Three analyses have compared the results digital and film hemispheric images. Englund *et al.* (2000) and Frazer *et al.* (2001) found that digital imagery generally showed that canopies were more open than the same canopies evaluated with film. In both of these studies, the canopy openness was relatively low – 8 percent for Englund and 35 percent for Frazer. A third analysis (Hale and Edwards, 2002) found a strong positive correlation between the results from the film and digital images and similar values for the several hemispheric measures examined, with no systematic differences over a range of transmittance from 10 to 70 percent. While this issue is cast in terms of digital versus film, differences in lenses used on the two classes of cameras may play a more important role in the differences noted than the media on which the image is captured. This issue warrants additional consideration but may become moot as the evolution of digital cameras enables them to utilize the hemispheric lenses that have been available only for film cameras.

Much of the work using hemispheric analysis is derived from forested settings. Our results are derived from riparian settings. In our images there is typically a substantial gap at high zenith angles as illustrated in Figure 1. Our results about sampling and analyst error may be dependent upon the configuration of these gaps and may not be applicable to settings with more homogenous cover.

One alternative to the use of hemispheric images is the use of a Solar Pathfinder, which is essentially a manual analogue approach to evaluating solar exposure. This is the device used in some previous work evaluating the role of solar exposure in stream ecosystems (e.g., Platts *et al.,* 1987; Platts and Nelson, 1989; Tait *et al.,* 1994, Maloney *et al.,* 1999). Swenson and Beilfuss (2001) compare the merits of the solar pathfinder to the analysis of hemispheric images collected with a film camera. They examined metrics similar to our DAYMay, DAYJune, DAYJuly and found a strong linear correlation with a slope of one between estimates derived from the two methods. They note that while "the Solar Pathfinder can be operated effectively in any weather condition, it is best suited for overcast days to avoid staring at the sun's reflected image" in the instrument. They note the value of the permanent record provided by the hemispheric image and raise concerns about the subjectivity of film exposure differences and scanned image inaccuracies. Our quantification of analyst error and sampling error helps to quantify the magnitude of these concerns in a digital system. They found that it took 13 to 15 minutes to process each image. This is in contrast to our experience of about three minutes per image; this difference is likely attributable to our use of a digital camera. Thus while the Solar Pathfinder is a viable alternative to hemispheric imagery, the time savings associated with the use of a digital system in comparison to the film system in their study is an argument in favor of the use of hemispheric images to quantify solar exposure.

Although it measures canopy closure, the densiometer is widely used to quantify stream solar exposure. The strong correlations between densiometer readings and hemispheric metrics (Table 3 and Figure 2) help to explain why densiometer readings have been useful in so many analyses (e.g., Herlihy *et al.,* 1998; Hill *et al.,* 1998; Bryce *et al.,* 1999; Pan *et al.,* 1999). At the same time, the uncertainty about these correlations represents the additional role that solar exposure may have in determining stream processes that are not captured in densiometer readings.

CONCLUSION

National stream monitoring and assessment programs evaluate stream solar exposure by measuring canopy closure rather than solar exposure. In this analysis we document a methodology that can characterize stream solar exposure. These improved metrics

enable a more thorough and mechanistic evaluation of the linkage between solar input and instream metrics. Thus, we recommend the use of hemispheric imagery for researchers who seek to evaluate the relationship between solar exposure and stream condition. An example of the type of evaluation that needs to be conducted before these methods should be adopted for more routine use is presented in Platts and Nelson (1989), which compares the value of a set of riparian closure and shading metrics and their relationship with salmonid biomass.

ACKNOWLEDGMENTS

We thank Jerry Clinton, Andrew Gray, Steve Cline and Gwendolyn Bury, who in addition to three of the coauthors of this paper served as image analysts for the section of this paper that compares the results of different analysts. We also thank Mike Bollman, Aaron Boriskeno, Sandy Bryce, Steve Cline, Mary Kentula, Pete Lattin, and Thomas Lossen for their efforts in collecting the data analyzed in this paper. Tim Lewis, Gordon Frazer, Rob Davies-Colley, and three anonymous reviewers graciously provided comments on drafts of this manuscript that resulted in substantial improvements. The information in this document has been funded wholly or in part by the U.S. Environmental Protection Agency. It has been subjected to review by the National Health and Environmental Effects Research Laboratory's Western Ecology Division and approved for publication. Approval does not signify that the contents reflect the views of the agency, nor does mention of trade names or commercial products constitute endorsement or recommendation for use.

LITERATURE CITED

Beschta, R. L., B. Bilby, G. W. Brown, L. B. Holtby, and T. D. Hofstra, 1987. Stream Temperature and Aquatic Habitat: Fisheries and Forestry Interactions. *In:* Streamside Management: Forestry and Fishery Interactions, E. O. Salo and T. W. Cundy (Editors). University of Washington, Seattle, Washington, pp. 191-232.

Bryce, S. A., D. P. Larsen, R. M. Hughes, and P. R. Kaufmann, 1999. Assessing Relative Risks to Aquatic Ecosystems: A Mid-Appalachian Case Study. Journal of the American Water Resources Association (JAWRA) 35(1):23-36.

Cairns, J., P. McCormick, and B. Niederlehner, 1993. A Proposed Framework for Developing Indicators of Ecosystem Health. Hydrobiologia 263:1-44.

Chazdon, R. L. and C. B. Field, 1987. Photographic Estimation of Photosynthetically Active Radiation: Evaluation of a Computerized Technique. Oecologia 73:525-532.

Chen, J., P. Rich, S. Gower, J. Norman, and S. Plummer, 1997. Leaf Area Index of Boreal Forests: Theory, Techniques, and Measurements. Journal of Geophysical Research-Atmospheres 102:29429-29443.

Comeau, P., F. Gendron, and T. Letchford, 1998. A Comparison of Several Methods for Estimating Light Under a Paper Birch Mixedwood Stand. Canadian Journal of Forest Research 28:1843-1850.

Cummins, K. W., G. W. Minshall, J. R. Sedell, C. E. Cushing, and R. C. Petersen, 1984. Stream Ecosystem Theory. Verh. Internat. Verein. Limnol. 22:1818-1827.

Davies-Colley, R. J. and G. W. Payne, 1998. Measuring Stream Shade. Journal of the North American Benthological Society 17:250-260.

Delta-T Devices, 1998. Hemiview User Manual Version 2.1. Delta-T Devices, Cambridge, United Kingdom, 79 pp.

Easter, M. J. and T. A. Spies, 1994. Using Hemispherical Photography for Estimating Photosynthetic Photon Flux Density Under Canopies and in Gaps in Douglas-Fir Forests of the Pacific Northwest. Canadian Journal of Forest Research 24:2050-2058.

Engelbrecht, B. and H. Herz, 2001. Evaluation of Different Methods to Estimate Understorey Light Conditions in Tropical Forests. Journal of Tropical Ecology 17:207-224.

Englund, S. R., J. J. O'Brien, and D. B. Clark, 2000. Evaluation of Digital and Film Hemispherical Photography and Spherical Densiometry for Measuring Forest Light Environments. Canadian Journal of Forest Research 30:1999-2005.

Feminella, J. W., M. E. Power, and V. H. Resh, 1989. Periphyton Responses to Invertebrate Grazing and Riparian Canopy in Three Northern California Coastal Streams. Freshwater Biology 22:445-457.

Ferment, A., N. Picard, S. Gourlet-Fleury, and C. Baraloto, 2001. A Comparison of Five Indirect Methods for Characterizing the Light Environment in a Tropical Forest. Annals of Forest Science 58:877-891.

Fisher, W., L. Jackson, G. Suter, and P. Bertram, 2001. Indicators for Human and Ecological Risk Assessment: A US Environmental Protection Agency Perspective. Human and Ecological Risk Assessment 7:961-970.

Fitzpatrick, F. A., I. Waite, P. J. D'Arconte, M. R. Meador, M. A. Maupin, and M. E. Gurtz, 1998. Revised Methods for Characterizing Stream Habitat in the National Water-Quality Assessment Program. U.S. Department of the Interior, U.S. Geological Survey, Water Resources Division, Raleigh, North Carolina, 67 pp.

Frazer, G. W., R. A. Fournier, J. A. Trofymow, and R. J. Hall, 2001. A Comparison of Digital and Film Fisheye Photography for Analysis of Forest Canopy Structure and Gap Light Transmission. Agricultural and Forest Meteorology 109:249-263.

Frazer, G. W., J. A. Trofymow, and K. P. Lertzman, 1997. A Method for Estimating Canopy Openness, Effective Leaf Area Index, and Photosynthetically Active Photon Flux Density Using Hemispherical Photography and Computerized Image Analysis Techniques. Information Report BC-X-373, Canadian Forest Service, Forest Ecosystem Processes Network, Pacific Forestry Centre, Natural Resources Canada, Victoria, British, Columbia, 73 pp.

Gregory, S. V., 1980. Effects of Light, Nutrients and Grazing on Periphyton Communities in Streams. Doctoral Thesis, Oregon State University, Corvallis, Oregon.

Grether, G., D. Millie, M. Bryant, D. Reznick, and W. Mayea, 2001. Rain Forest Canopy Cover, Resource Availability, and Life History Evolution in Guppies. Ecology 82:1546-1559.

Hale, S. E. and C. Edwards, 2002. Comparison of Film and Digital Hemispherical Photography Across a Wide Range of Canopy Densities. Agricultural and Forest Meteorology 112:51-56.

Herlihy, A. T., J. L. Stoddard, and C. B. Johnson, 1998. The Relationship Between Stream Chemistry and Watershed Land Cover Data in the Mid-Atlantic Region, USA. Water, Air and Soil Pollution 105:377-386.

Hill, B. H., A. T. Herlihy, P. R. Kaufman, and R. L. Sinsabaugh, 1998. Sediment Microbial Respiration in a Synoptic Survey of Mid-Atlantic Region Streams. Freshwater Biology 39:493-501.

Jackson, L. E., J. C. Kurtz, and W. S. Fisher, 2000. Evaluation Guidelines for Ecological Indicators. EPA/620/R-99/005, U.S. Environmental Protection Agency, Office of Research and Development, Research Triangle Park, North Carolina, 107 pp.

Jennings, S., N. Brown, and D. Sheil, 1999. Assessing Forest Canopies and Understorey Illumination: Canopy Closure, Canopy Cover and Other Measures. Forestry 72:59-74.

Kaufmann, P. R., P. Levine, E. G. Robison, C. Seeliger, and D. V. Peck, 1999. Quantifying Physical Habitat in Wadeable Streams. EPA/620/R-99/003, U.S. Environmental Protection Agency, Washington, D.C., 125 pp.

Lieffers, V., C. Messier, K. Stadt, F. Gendron, and P. Comeau, 1999. Predicting and Managing Light in the Understory of Boreal Forests. Canadian Journal of Forest Research 29:796-811.

Machado, J. and P. Reich, 1999. Evaluation of Several Measures of Canopy Openness as Predictors of Photosynthetic Photon Flux Density in Deeply Shaded Conifer-Dominated Forest Understory. Canadian Journal of Forest Research 29:1438-1444.

Maloney, S. B., A. R. Tiedemann, D. A. Higgins, T. M. Quigley, and D. B. Marx, 1999. Influence of Stream Characteristics and Grazing Intensity on Stream Temperatures in Eastern Oregon. PNW-GTR-459, USDA Forest Service, Pacific Northwest Research Station. Portland, Oregon, 19 pp.

Miller, Jr., R. G., 1986, Beyond ANOVA, Basics of Applied Statistics. John Wiley and Sons, New York, New York.

Pan, Y., R. J. Stevenson, B. H. Hill, P. R. Kaufman, and A. T. Herlihy, 1999. Spatial Patterns and Ecological Determinants of Benthic Algal Assemblages in Mid-Atlantic Highland Streams, USA. Journal of Phycology 35:460-468.

Peck, D. V., J. Lazorchak, and D. Klemm, 2000. Environmental Monitoring and Assessment Program - Surface Waters: Western Pilot Study: Field Operations Manual for Wadeable Streams. Washington, D.C., 226 pp. *Available at* http://www.epa.gov/emap/html/pubs/docs/groupdocs/surfwatr/field/ewwsm01.html. *Accessed in* October 2003.

Platts, W. S., S. C. Armour, G. D. Booth, M. Bryant, J. L. Bufford, P. Cuplin, S. Jensen, G. W. Lienkaemper, G. W. Minshall, G. W.Monsen, S. B. Monsen, R. L.Nelson, J. R. Sedell, and J. S. Tuhy, 1987. Methods for Evaluating Riparian Habitats with Applications to Management. General Technical Report INT-221, USDA-FS, Intermountain Forest and Range Experiment Station, Ogden Utah, 177 pp.

Platts, W. S., W. F. Megahan, and G. W. Minshall, 1983. Methods for Evaluating Stream, Riparian, and Biotic Conditions. General Technical Report INT-183, USDA Forest Service, Washington, D.C.

Platts, W. S. and R. L. Nelson, 1989. Stream Canopy and Its Relationship to Salmonid Biomass in the Intermountain West. North American Journal of Fisheries Management. 9:446-457.

Regent Instruments, 1999. Winscanopy. *Available at* http://www.regent.qc.ca/products/Brochures/WinSCANOPY.pdf. *Accessed on* October 2003.

Rich, P. M., 1990. Characterizing Plant Canopies With Hemispherical Photographs. Remote Sensing Reviews 5:13-29.

Robison, S. and B. McCarthy, 1999. Potential Factors Affecting the Estimation of Light Availability Using Hemispherical Photography in Oak Forest Understories. Journal of the Torrey Botanical Society 126:344-349.

Roxburgh, J. and D. Kelly, 1995. Uses and Limitations of Hemispherical Photography for Estimating Forest Light Environments. New Zealand Journal of Ecology 19:213-217.

Rutherford, J. C., R. J. Davies-Colley, J. M. Quinn, M. J. Stroud, and A. B. Cooper, 1999, Stream Shade: Towards a Restoration Strategy. National Institute of Water and Atmospheric Research (NIWA) and Department of Conservation, Wellington, New Zealand.

Shaw, D. C. and K. Bible, 1996. An Overview of Forest Canopy Ecosystem Functions With Reference to Urban and Riparian Systems. Northwest Science 70:1-6.

Sokal, R. R. and F. J. Rohlf, 1981, Biometry. W. H. Freeman, San Francisco, California.

Stevens, Jr., D. L., 1997. Variable Density Grid-Based Sampling Designs for Continuous Spatial Populations. Environmetrics 8:167-195.

Stevens, Jr., D. L. and A. R. Olsen, 1999. Spatially Restricted Surveys Over Time for Aquatic Resources. Journal of Agricultural, Biological, and Environmental Statistics 4:415-428.

Swenson, S. and R. Beilfus, 2001. Calculating Light Levels for Savanna and Woodland Restorations: Solar Pathfinder or Computerized Analysis of Hemispherical Photographs? Ecological Restoration 19:161-164.

Tait, C. K., J. L. Li, G. A. Lamberti, T. N. Pearsons, and H. W. Li, 1994. Relationships Between Riparian Cover and the Community Structure of High Desert Streams. Journal of the North American Benthological Society 13:45-56.

U.S. Bureau of Reclamation, 2001. The Pacific Northwest Cooperative Agricultural Weather Network, U.S. Department of the Interior Bureau of Reclamation Pacific Northwest Region. *Available at* http://www.usbr.gov/pn/agrimet/. *Accessed in* October 2003.

Whitmore, T., N. Brown, M. Swaine, D. Kennedy, C. Goodwinbailey, and W. Gong, 1993. Use of Hemispherical Photographs in Forest Ecology - Measurement of Gap Size and Radiation Totals in a Bornean Tropical Rain Forest. Journal of Tropical Ecology 9:131-151.